

Low-temperature thermal conductivity in polycrystalline graphene

D.V. Kolesnikov, V.A. Osipov

*Bogoliubov Laboratory of Theoretical Physics,
Joint Institute for Nuclear Research,
141980 Dubna, Moscow region, Russia*

(Dated: April 24, 2021)

Abstract

The low-temperature thermal conductivity in polycrystalline graphene is theoretically studied. The contributions from three branches of acoustic phonons are calculated by taking into account scattering on sample borders, point defects and grain boundaries. Phonon scattering due to sample borders and grain boundaries is shown to result in a T^α -behaviour in the thermal conductivity where α varies between 1 and 2. This behaviour is found to be more pronounced for nanosized grain boundaries.

65.80.Ck Thermal properties of graphene

81.05.ue Graphene

73.43.Cd Theory and modeling

I. INTRODUCTION

The thermal conductivity of both single-layer and few-layer graphene is of current experimental and theoretical interest (see a recent review [1] and the references therein). It was shown that the heat conduction in graphene has a specific behaviour due to the unique nature of two-dimensional phonons. Main attention has been attracted to studies of the heat transfer in graphene near room temperature because of possible applications in electronics and photonics.

In this paper, we focus on the thermal conductivity in graphene at low temperatures. Our interest is stimulated by recent observations that the large-scale graphene films are typically polycrystalline [2–5] and consist of many single-crystalline grains separated by grain boundaries (GB) [6–8]. The grain sizes are dependent on growth conditions, ranging from hundreds of nanometres to tens of micrometres for slight changes in growth conditions [6]. Recently, the fabrication of nanocrystalline graphene made by electron-radiation induced cross-linking of aromatic self-assembled monolayers and their subsequent annealing was reported [9]. Nanosized grain boundary loops originating from paired five- and seven-membered ring disclinations were observed and analysed in [10].

The GB-induced phonon scattering has a marked impact on the thermal conductivity, κ , at low temperatures. In bulk materials, the well-pronounced crossover from $\kappa \sim T^2$ to $\kappa \sim T^3$ has been proved with the crossover temperature strongly depending on the GB size [11, 12]. Therefore, one can expect a similar effect in two-dimensional polycrystalline materials like graphene. The paper is organized as follows. In Section 2 we overview the general formalism with three main acoustic phonon branches taken into account: longitudinal (LA), transverse (TA) and flexural (ZA). The effective temperatures characterizing the phonon mean free paths for main scattering mechanisms are introduced. The results of numerical calculations of the thermal conductivity are presented in section 3. Conclusion is devoted to the discussion of the results obtained.

II. GENERAL FORMALISM

According to [13], the phonon thermal conductivity of single-layer graphene can be written as

$$\kappa = \frac{1}{4\pi k_B T^2 h_{eff}} \sum_s \int_0^{q_D} (\hbar\omega_s(q))^2 v_s(q) l_s(q, T) \times \frac{e^{\hbar\omega_s(q)/(k_B T)}}{(e^{\hbar\omega_s(q)/(k_B T)} - 1)^2} q dq, \quad (1)$$

where summation is performed over the phonon polarization branches with the dispersion relations $\omega_s(q)$ (q is the wavevector, q_D corresponds to the edge of the Brillouin zone, and s is the branch index), h_{eff} is the effective graphene layer thickness, $v_s(q) = \partial\omega_s(q)/\partial q$ is the phonon group velocity, $l_s(q, T)$ is the phonon mean free path, and k_B is the Boltzmann constant. The phonon mean free path, l_s , is limited by three major independent scattering mechanisms: sample borders (rough boundary (RB)), point defect (PD), and grain boundary. Within the relaxation-time approximation, it reads

$$1/l_s = 1/l_0 + 1/l_{PD} + 1/l_{GB}, \quad (2)$$

where l_0 , l_{PD} and l_{GB} comes from phonon scattering by RB, PD, and GB, respectively. The phonon-RB scattering is given by [15]

$$l_0^{-1} = \frac{1}{d} \frac{1-p}{1+p}, \quad (3)$$

with p being the specularity parameter defined as a probability of specular scattering at the sample borders and d the graphene layer size. The phonon-PD scattering can be written as

$$l_{PD}^{-1} = \frac{S_0 \Gamma}{4} \frac{q(\omega)}{v^2(\omega)} \omega^2, \quad (4)$$

where S_0 is the cross-section area per one atom of the lattice and Γ is the measure of the scattering strength. It was suggested in [16] that grain boundaries can be naturally described by disclinations. In graphene, the alternating pentagon-heptagon structure along high-angle GBs was revealed in [8]. This finding allows us to model the grain boundary by biaxial wedge disclination dipole (BWDD) of length \mathcal{L} which consists of 5-7 pairs (see Fig. 1). In this case, the phonon-GB scattering can be expressed as [11]

$$l_{GB}^{-1} = 2D^2(\nu\mathcal{L})^2 n_i q \mathcal{G}(q\mathcal{L}), \quad (5)$$

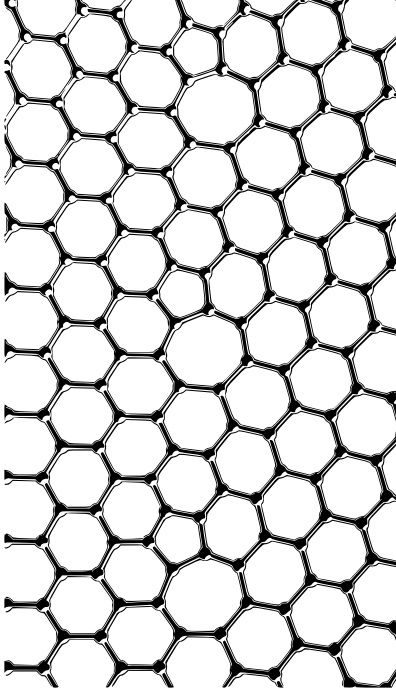


FIG. 1. The fragment of grain boundary in polycrystalline graphene. The size \mathcal{L} of this wall exceeds eight lattice translations. Notice that the whole wall corresponds to a single BWDD.

where ν is the Frank index, n_i is the areal density of BWDDs,

$$\mathcal{G}(z) = J_0^2(z) + J_1^2(z) - J_0(z)J_1(z)/z,$$

$J_i(z)$ is the Bessel functions of i th kind, and

$$D = \pi\gamma(1 - 2\sigma)/(1 - \sigma), \quad (6)$$

where γ is the Gruneisen constant of a given phonon branch and σ is the Poisson constant (see [11, 12] for detail).

Generally, there are six phonon branches. However, at low temperatures only three branches are of importance: acoustic longitudinal (LA) and transversal (TA) phonons with the ordinary dispersion relation $\omega_s = v_s q$ ($s = LA, TA$) and out-of-plane (flexural) acoustic phonon branch (ZA) with $\omega_{ZA} = q^2/2m$, where $m = 2\sqrt{\rho_{2D}/K}$ is an effective parameter [14], ρ_{2D} and K are graphene 2D mass density and bending stiffness, respectively. Notice that at sufficiently low temperatures the umklapp processes of phonon-phonon scattering are mainly frozen and can be neglected.

Let us introduce the dimensionless parameter x , $x = \hbar\omega/(k_B T)$. For LA and TA phonons

eq.(1) takes the form

$$\kappa_s = \frac{C_s T^2}{h_{eff}} \int_0^{\theta_D/T} \lambda_s(x, T) \frac{x^3 e^x dx}{(e^x - 1)^2}, \quad (7)$$

where θ_D is the Debye temperature, $C_s = k_B^3 l_0 / (4\pi \hbar^2 v_s)$, and

$$\lambda_s^{-1}(x, T) = 1 + \left(x \frac{T}{T_{PD}}\right)^3 + x \frac{T}{T_{GB}} \mathcal{G}\left(x \frac{T}{T_0}\right) \quad (8)$$

is the total mean free path normalized to l_0 ($\lambda_s = l_s/l_0$). As a matter of convenience we have introduced here three characteristic temperatures:

$$T_{PD} = \frac{\hbar v_s}{k_B} \left(\frac{4}{S_0 \Gamma l_0}\right)^{1/3} \quad (9)$$

for PD scattering,

$$T_0 = \frac{\hbar v_s}{\mathcal{L} k_B}, \quad (10)$$

and $T_{GB} = \hbar v_s / (2D^2 \nu^2 \mathcal{L}^2 k_B l_0 n_i)$ for GB scattering. In order to clarify the role of the GB scattering let us temporary disregard the second term in eq. (8) which is responsible for PD scattering. In this case, $l_s \approx l_0 (1 + 2T_0 / (\pi T_{GB}) + \mathcal{O}(T_0^3 / (T_{GB} T^2)))^{-1}$ for $xT \gg T_0$ (the short wavelength limit). As is shown below, typically $T_0 > T_{GB}$. Therefore, namely T_0 defines the region of marked influence of phonon-GB scattering and can be considered as a threshold temperature. It should be also mentioned that T_0 characterizes the temperature when the wavelength of an incident phonon becomes comparable with the size of grain boundary.

To take into account the imperfect packing of grains one can introduce the average distance between grain boundaries, a , so that the areal density of grains is estimated as $n_i = (a + \mathcal{L})^{-2}$ and

$$T_{GB} = \frac{\hbar v_s (1 + a/\mathcal{L})^2}{2D^2 \nu^2 k_B l_0}, \quad (11)$$

where $(1 + a/\mathcal{L})^{-2}$ is a packing coefficient. Notice that while T_{GB} depends on a/\mathcal{L} , T_0 is a function of \mathcal{L} only.

The heat conductivity due to ZA phonons is written as

$$\kappa_{ZA} = \frac{C_{ZA} T^{3/2}}{h_{eff}} \int_0^{\theta_{ZA}/T} \lambda_{ZA}(x, T) \frac{x^{5/2} e^x dx}{(e^x - 1)^2}, \quad (12)$$

where $C_{ZA} = \sqrt{2m} k_B^{5/2} l_0 / (4\pi \hbar^{3/2})$ and

$$\begin{aligned} \lambda_{ZA}^{-1}(x, T) = 1 + \gamma_{ZA}^2(x, T) & \left(\left(x \frac{T}{T_{PD}}\right)^{3/2} + \right. \\ & \left. + \sqrt{x \frac{T}{T_{GB}}} \mathcal{G}\left(\sqrt{x \frac{T}{T_0}}\right) \right). \end{aligned} \quad (13)$$

The characteristic temperature of PD scattering takes the form

$$T_{PD} = \frac{1}{m} \left(\frac{4\sqrt{2}}{S_0\Gamma l_0} \right)^{2/3} \frac{\hbar}{k_B}, \quad (14)$$

while for GB scattering one obtains $T_0 = \hbar/(2\mathcal{L}^2mk_B)$ and

$$T'_{GB} = \frac{\hbar(1+a/\mathcal{L})^4}{8mk_B[D'^2\nu^2l_0]^2}, \quad (15)$$

where $D' = \pi(1 - 2\sigma)/(1 - \sigma)$. Notice that the Gruneisen constant for ZA phonons $\gamma(q)$ is assumed to depend on the wavevector q in contrast to LA/TA cases. In accordance with [19] one can use an approximate expression $\gamma_{ZA}(q) = -1 - 80(q/q_D - 1)^2$ or, equivalently,

$$\gamma_{ZA}(x, T) = -1 - 80\left(\sqrt{x\frac{T}{\theta_{ZA}}} - 1\right)^2. \quad (16)$$

III. RESULTS

The total phonon thermal conductivity of graphene is calculated by using eqs. (7) and (12). The major initial parameters used in the model are $d = 5\mu m$, $p = 0.9$, $v_{LA} = 21.3km/s$, $v_{TA} = 13.6km/s$ (from [13]), $\gamma_{LA} = 1.8$, $\gamma_{TA} = 0.75$ (from [1]), and $\gamma_{ZA}(x, T)$ determined by eq. (16) (which approximates the dependence of Gruneisen constant for ZA branch on the wavevector), as well as $m = 1.0 \cdot 10^6 s/m^2$ are taken from [19]. One should note, that the Gruneisen parameter for the ZA phonon branch is varying within the Brilluoin zone by the order of several magnitudes, in contrast with LA and TA cases. To take into account the influence of ZA phonons, we use eq. (16) for the Gruneisen parameter instead of constant value. We use the upper limit for the specular graphene thickness parameter $h_{eff} = 0.69nm$ from [24]. One should also note that the differences in the recent theoretical and experimental models give rise to the discrepancy in the determination of certain graphene constants (see the discussion in [1] for detail). However, this discrepancy will not play crucial role for the effects discussed below.

Using the constants defined above, one obtains $C_{LA} = 8.40 \cdot 10^{-11}W/K^3$, $C_{TA} = 1.31 \cdot 10^{-10}W/K^3$, $C_{ZA} = 5.93 \cdot 10^{-9}W/K^{5/2}$. The characteristic temperatures are given in tables I and II. We restrict our consideration to the temperatures below 100 K. To estimate the parameter T_{PD} we fit our model in the case of graphene single crystal according to the results of [13]. We found that T_{PD} exceeds 100K for the leading phonon modes, and thus PD scattering turns out to be of little consequence within the temperature interval considered.

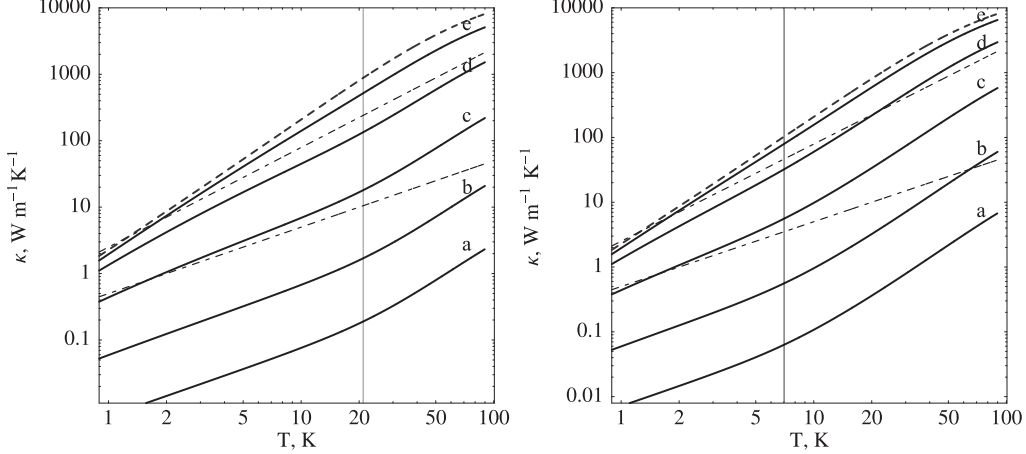


FIG. 2. The total thermal conductivity of polycrystalline graphene with high-angle grain boundaries for $\mathcal{L} = 2.46\text{nm}$ (left) and $\mathcal{L} = 7.38\text{nm}$ (right) at different packing coefficients: (a) $a/\mathcal{L} = 0$, (b) $a/\mathcal{L} = 2$, (c) $a/\mathcal{L} = 9$, (d) $a/\mathcal{L} = 30$, and (e) $a/\mathcal{L} = 100$ (see table II). Dashed curve corresponds to a case of graphene single crystal. Dot-dashed straight lines shows $T^{1.5}$ and T . The approximate crossover temperatures are indicated with vertical lines.

Fig.2 shows the thermal conductivity of graphene as a function of temperature for $\mathcal{L} = 2.46\text{ nm}$ and $\mathcal{L} = 7.38\text{ nm}$ at different packing. For comparison, the dot-dashed lines shows the functions $T^{1.5}$ and T , while the dashed curve corresponds to a case of graphene single crystal. The thermal conductivity of the graphene single crystal follows a square law in a wide temperature region excepting the very low temperatures where κ_{ZA} has a marked impact and high temperatures (in the range of $80 - 100\text{ K}$) where PD scattering has a slight influence.

For polycrystalline graphene, one can clearly see the characteristic points where crossover occurs. The crossover temperature is estimated as $T^* \approx T_0/2$, where T_0 is governed by the dominant phonon mode, (TA). Above T^* the thermal conductivity behaves like T^2 while below T^* the behaviour is acutely sensitive to T_{GB} (see eq. (11)). In turn, T_{GB} depends distinctly on the packing coefficient and GB's angle. Notice that high-angle GBs with $\nu \approx 0.083$ were revealed in [8]. For this case, the typical values of T_{GB} at different packing coefficients are shown in table II. At low T_{GB} one obtains $\kappa \sim T$ while growing T_{GB} results in $\kappa \sim T^{1.5}$ and, finally, in $\kappa \sim T^2$. One can conclude that the lower is T_{GB} , the more pronounced influence of grain boundaries takes place.

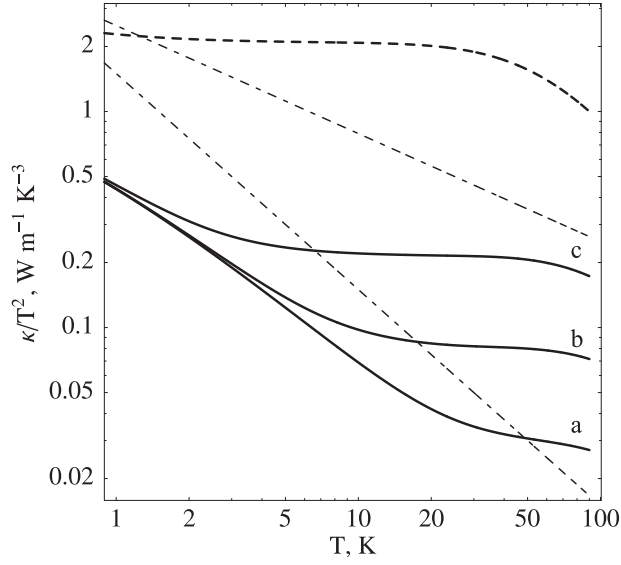


FIG. 3. Reduced thermal conductivity, κ/T^2 , versus temperature T for a graphene single crystal (dashed) and polycrystalline graphene (solid) at fixed packing coefficient $a/\mathcal{L} = 9$ and different grain sizes: (a) $\mathcal{L} = 2.46\text{nm}$, (b) $\mathcal{L} = 7.38\text{nm}$, and (c) $\mathcal{L} = 22.14\text{nm}$. Dot-dashed straight lines shows $T^{1.5}$ and T .

TABLE I. The threshold temperature at different grain sizes for three phonon branches.

\mathcal{L} , nm	2.46	7.38	22.14
T_0, K (LA)	66.0	22.0	7.33
T_0, K (TA)	42.1	14.0	4.68
T_0, K (ZA)	0.6	0.066	0.0074

Fig. 3 shows reduced thermal conductivity, κ/T^2 , versus temperature at fixed packing coefficient. As is clearly seen, both the thermal conductivity and the crossover temperature decreases with increasing GB size. In case of graphene single crystal, one can mention once again a slight deviation from a T^2 -behaviour due to the influence of ZA phonons. Point defects are responsible for deviations at high temperatures.

TABLE II. The grain boundary temperature at different effective distances between grains for the case of high-angle grain boundaries ($\nu = 1/12$).

a/\mathcal{L}	0.0	2.0	9.0	30.0	100.0
T_{GB}, mK (LA)	1.5	13.5	149.7	1438.9	15273.6
T_{GB}, mK (TA)	5.5	49.5	550.6	5291.8	56172.5
T'_{GB}, mK (ZA)	$1.3 \cdot 10^{-7}$	$1.06 \cdot 10^{-5}$	0.0013	0.12	13.63

IV. CONCLUSION

In this paper, the influence of polycrystalline structure on the low-temperature heat transfer in suspended graphene has been theoretically studied. Three acoustic phonon branches were taken into account and three types of scattering mechanisms were discussed: sample boundary scattering, point defects and phonon scattering on the grain boundaries. The rough-boundary scattering is found to play an important role over the whole considered temperature range (0-100 K). On the contrary, the point defect scattering manifests itself only at the upper limit of the temperature interval. The influence of polycrystalline structure is described by two temperature parameters T_{GB} and T_0 which, in turn, define the crossover temperature T^* . Above T^* , the heat conductivity behaves like in graphene single crystal, $\kappa \sim T^2$, with an adjusted rough-boundary scattering parameter. Below the crossover point we found that $\kappa \sim T^\alpha$ where α values range from 1 to 2 with increasing T_{GB} . In experiment, such behaviour of the thermal conductivity could be a manifestation of the grain-boundary scattering mechanism. T_{GB} decreases with an increase of the packing coefficient, the misorientation angle and/or a sample size while T_0 depends on the grain boundary length only.

In our study, the contribution of TA phonons is found to be dominant. The contribution of LA phonon branch is suppressed due to the higher (in comparison to TA) sound velocity while ZA phonons are of little importance due to the large Gruneisen constant. To be more precise, in our consideration ZA phonons manifests themselves only at very low temperatures and the grain-boundary scattering additionally suppresses their influence.

It is interesting to note that in some recent experiments with suspended single-layer [20, 21] and few-layer [22] graphene the temperature dependence of κ was found to follow a power law with an exponent of 1.4 ± 0.1 . This behaviour can be attributed to a dominant

contribution from the ZA phonon modes. However, the measured thermal conductivity in those samples are much lower compared to the theoretically expected values. As possible alternative explanations one considers scattering of phonons in the bilayer graphene by a residual polymeric layer, a high concentration of defects due to processing [23], or the polycrystalline structure of graphene with small and misoriented grains [24]. In this article we have shown that the phonon-GB scattering will objectively result in T^α behaviour of thermal conductivity with $1 < \alpha \leq 2$.

This work has been supported by the Russian Foundation for Basic Research under grant No. 12-02-01081.

-
- [1] D.L. Nika and A.A. Balandin *J. Phys.: Condens. Matter* 24, 233203(2012)
 - [2] X.S. Li et al. *Nano Lett.* 10, 43284334(2010)
 - [3] O.V. Yazyev and S.G. Louie *Phys. Rev. B* 81, 195420(2010)
 - [4] O.V. Yazyev and S.G. Louie *Nature Mat.* 9, 806(2010)
 - [5] J. da Silva Araujo and R.W. Nunes *Phys. Rev. B* 81, 073408(2010)
 - [6] P. Y. Huang et. al. *Nature* 469, 389(2011)
 - [7] J. Lahiri et. al. *Nat. Nanotechnol.* 5, 326(2010)
 - [8] K.Kim et. al. *ACS NANO* 5, 2142(2011)
 - [9] A. Turchanin et. al. *ACS NANO* 5, 3896(2011)
 - [10] E.Cockayne et. al. *Phys. Rev. B* 83, 195425(2011)
 - [11] V.A. Osipov and S.E.Krasavin *J.Phys.:Condens. Matter* 10, L639(1998)
 - [12] S.E.Krasavin and V.A.Osipov *J.Phys.:Condens. Matter* 13, 1023(2001)
 - [13] D.L.Nika, E.P.Pokatilov, A.S.Askerov and A.A.Balandin *Physical Review B* 79, 155413(2009)
 - [14] A. H. Castro Neto et. al. *Rev. Mod. Phys* 81, 109(2009)
 - [15] J.M. Ziman *Electrons and Phonons: The Theory of Transport Phenomena in Solids*, Clarendon, Oxford (1960)
 - [16] J.C.M. Li *Surf. Sci.* 31, 12(1972)
 - [17] A.Fasolino, J.H.Los and M.I.Katsnelson *Nature Materials* 6, 858(2007)
 - [18] D. L. Nika et. al. *Appl. Phys. Lett.* 94, 203103(2009)

- [19] Nicolas Mounet and Nicola Marzari Phys. Rev. B 71, 205214(2005)
- [20] X.Xu et. al. arXiv:1012.2937(2010)
- [21] S.Liu et. al. arXiv:1205.3065(2012)
- [22] Z.Wang et. al. Nano Lett. 11 (1), 113(2011)
- [23] M.T. Pettes et. al. Nano Lett. 11, 1195(2011)
- [24] A.A. Balandin Nature Materials 10, 569581(2011)